Uncertainty in 21st century ocean temperature projections near Greenland

Christopher Little (cmlittle@princeton.edu) and Michael Oppenheimer
Department of Geosciences and Woodrow Wilson School of Public and International Affairs
Princeton University
GRISO workshop 2013

Background

Atmosphere-ocean general circulation models (AOGCMs) do not resolve small-scale processes near ice sheet margins. For the purposes of projecting ocean-driven changes in the Greenland ice sheet's mass balance, these global models may be better used to inform the expected range of large-scale changes in ocean temperature; models that account for oceanic, atmospheric, and glaciological processes in fjords and outlet glaciers may be used to link far-field boundary conditions to ice dynamics. This strategy (analogous to the use of RCM's for ice sheet surface mass balance projections) requires choosing appropriate "source" regions in AOGCMs, and assessing uncertainty in ocean heat content in those regions.

Rignot et al. (2012) utilize a high-resolution model to illustrate that North Atlantic subpolar gyre (NASPG) temperature anomalies are transported rapidly along the pathways detailed in Straneo et al. (2012) (to right).

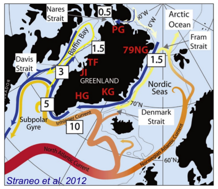

Straneo et al. 2012

In Rignot et al. (2012), "off-shelf" anomalies are shown to persist "on-shelf" (below).

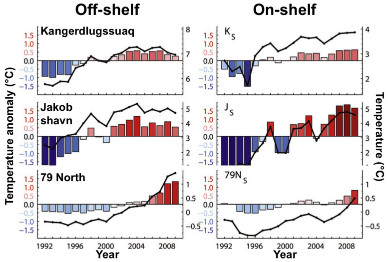

Modified from Rignot et al. 2012

These results suggest two choices for "source" regions: 1) at locations near individual outlet glaciers; 2) over the entire NASPG. Here, we analyze the range of 21st century ocean warming in these regions, projected using RCP simulations in the CMIP5 archive. Three 2°x2° "off-shelf" regions near Kangerdlugssuaq, Jakobshavn, and 79 North glaciers are selected (small black boxes). The NASPG is defined as the oceanic region between 50-64N and 0-60W (dark blue boxes).

Methods

We analyze the potential temperature field (thetao) from CMIP5 "historical" control runs and RCP simulations (http://cmip-pcmdi.llnl.gov/cmip5/). We use the set of model simulations shown in the table at right.

Ocean model output (at a variety of different resolutions and on native grids) is regridded to a 1x1 degree lat/lon grid. Gridpoints are included in the analysis if they include data from more than 3 models.

Historical bias is the difference in the multimodel mean potential temperature from the ECDA coupled model reanalysis (Chang et al. 2013) over each depth range. If multiple realizations of historical simulations are available, the mean of all realizations for that model is used.

For the RCP simulations, 10 year timeslices from 2050-2059 and 2090-2099 are extracted and regridded, and used to calculate anomalies ("warming") from 1980-2005 means.

Model	Hist	RCP 2.6	RCP 4.5	RCP 6.0	RCP 8.5
CCSM4	X				
CNRM-CM5	X				
CSIRO-Mk3.6	X				
FGOALS-g2	X				
FGOALS-s2	X				
GFDL-ESM2M	X	X	X	X	X
GFDL-ESM2G	X	X	X	X	X
GFDL-CM3	X	X	X	X	X
GISS-E2-R	X	X	X	X	
HadGEM2-ES	X	X	X	X	X
IPSL-CM5A-LR	X	X	X	X	X
IPSL-CM5A-MR	X	X	X		X
IPSL-CM5B-LR	X				
MIROC5	X	X	X	X	X
MIROC-ESM	X	X	X	X	X
MIROC-ESM-CHEM	X	X	X	X	X
MPI-ESM-LR	X	X	X		X
MPI-ESM-MR	X		X		X
MRI-CGCM3	X	X	X	X	X
NorESM1-M	X	X	X	X	X
NorESM1-ME	X	X	X	X	X
TOTAL	**21**	**14**	**15**	**12**	**14**

CMIP5 global surface warming projections for RCP scenarios. Multimodel mean projections are shown with solid lines; shading shows ±1 SD ranges.

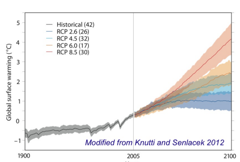

Modified from Knutti and Sedlacek 2012

RCP simulations to 2100

Multimodel mean warming (shading); Multimodel SD (contours)
(RCP 8.5; 0-500m mean temperature; °C)

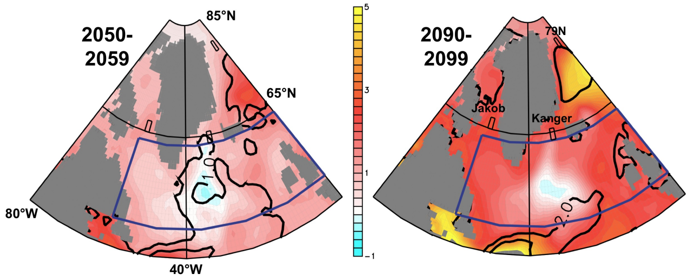

Depth-averaged ocean warming projections for the RCP 8.5 scenario. Multimodel mean warming is shaded, with warming in reds and yellows; multimodel SD is indicated with contours at 1°C intervals. The spatial patterns of warming/cooling are similar in all scenarios; quantities are relatively insensitive to depth.

Summary results (0-500m mean temperature, °C)

RCP	SPG (2050-2059)	Kanger (2050-2059)	Jakob (2050-2059)	79N (2050-2059)
2.6	0.4 ± 0.8	0.5 ± 0.6	0.8 ± 0.4	0.6 ± 0.4
4.5	0.5 ± 0.8	0.5 ± 0.5	0.9 ± 0.4	0.7 ± 0.5
6.0	0.5 ± 0.7	0.5 ± 0.5	0.9 ± 0.4	0.6 ± 0.4
8.5	0.7 ± 0.9	0.8 ± 0.6	1.2 ± 0.5	1.0 ± 0.6
ALL	**0.5 ± 0.8**	**0.6 ± 0.6**	**1.0 ± 0.4**	**0.7 ± 0.5**

RCP	SPG (2090-2099)	Kanger (2090-2099)	Jakob (2090-2099)	79N (2090-2099)
2.6	0.5 ± 0.8	0.5 ± 0.6	0.9 ± 0.4	0.8 ± 0.7
4.5	0.7 ± 1.0	0.8 ± 0.6	1.4 ± 0.5	1.3 ± 0.9
6.0	1.0 ± 1.1	1.2 ± 0.7	1.7 ± 0.8	1.4 ± 1.0
8.5	1.6 ± 1.3	2.1 ± 1.1	2.6 ± 1.0	2.4 ± 1.4
ALL	**0.9 ± 1.2**	**1.1 ± 1.0**	**1.6 ± 0.9**	**1.5 ± 1.2**

Depth-averaged ocean warming (departure from 1980-2005 mean) in the "source" region, at two different timeslices, for four RCP scenarios ($\mu_s \pm \sigma_s$; multimodel mean ± 1SD).

Multimodel mean

$$\mu_s = \frac{1}{N_m}\sum_{n=1}^{N_m}\theta(x,y,z,t,m)$$

Multimodel standard deviation

$$\sigma_s = \sqrt{\frac{1}{N_m}\sum_{n=1}^{N_m}(\theta_{m,s}-\mu_s)^2}$$

Partitioning uncertainty in projections

Model uncertainty (0-500m mean temperature, °C)

$$\sigma_m = \frac{1}{N_s}\sum_{n=1}^{N_s}\sigma_s$$

Scenario uncertainty (0-500m mean temperature, °C)

$$\bar{\sigma}_s = \frac{1}{N_s}\sum_{n=1}^{N_s}\sqrt{\frac{1}{N_s}\sum_{n=1}^{N_s}(\mu_s-\mu_{all})^2}$$

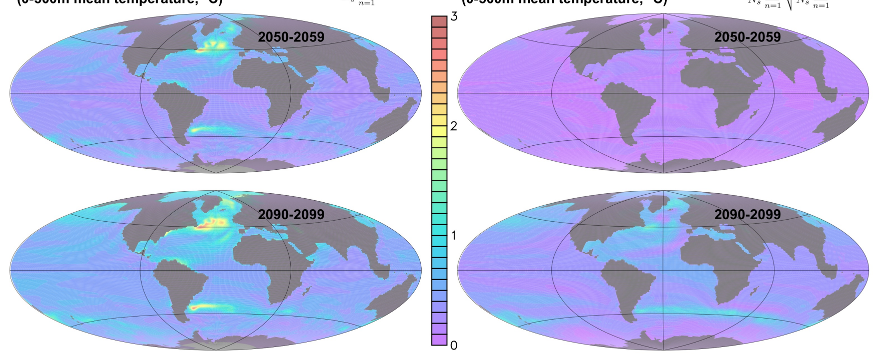

Model (left) and scenario (right) uncertainty, calculated using the above formulas. Results at different depth ranges between 0-500m are qualitatively similar.

1980-2005 mean temperature bias

Multimodel mean bias (shading); Multimodel SD (contours)
(depth-mean temperature, °C)

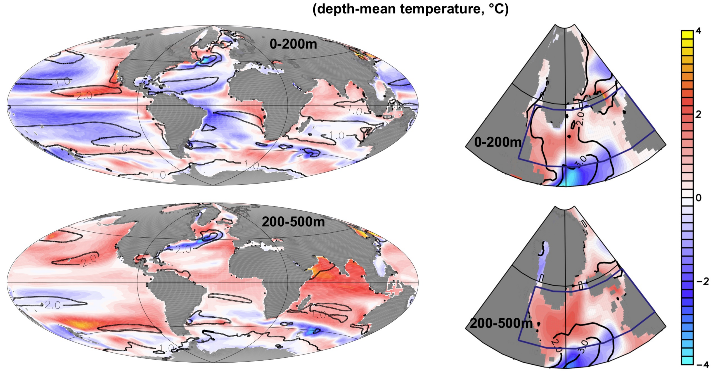

	Historical Bias 0-200m	Historical Bias 200-500m
SPG	0.4 ± 2.0	1.0 ± 1.7
Kanger	-0.2 ± 2.4	0.5 ± 1.6
Jakob	-0.4 ± 1.2	-0.5 ± 1.3
79N	0.3 ± 0.8	0.1 ± 1.3

Depth-averaged ocean temperature bias (departure from 1980-2005 mean value in the ECDA reanalysis) at different depths. A warm bias becomes more apparent at depth. Multimodel mean bias is shaded, with warming in reds and yellows; multimodel SD is indicated with contours at 1°C intervals. Variability across realizations from individual models is much lower than that across models.

Conclusions

- ☆ **Uncertainty in AOGCM projections of ocean temperature resulting from different RCPs (scenario, or forcing, uncertainty) is smaller than the inter-model spread (model, or structural, uncertainty), especially through the mid-21st century.**
- ☆ **Using a small subset of AOGCMs to develop forcing scenarios for ice sheet models is thus unadvisable.**
- ☆ **Model and scenario uncertainty in ocean temperature, and biases in historical runs, reach their global maxima in the North Atlantic subpolar gyre (NASPG).**
- ☆ **The expected ocean warming rates are larger and the inter-model spread is reduced closer to Greenland.**
- ☆ **These findings suggest: 1) counter-intuitively, projections of ocean forcing of the Greenland ice sheet are more robust at small(er) scales, closer to outlet glaciers; 2) observed decadal variability in ocean heat content (e.g. the mid-1990's warming of the NASPG) may not be analogous to the century-timescale changes projected by AOGCM's.**

Model:Scenario uncertainty ratio

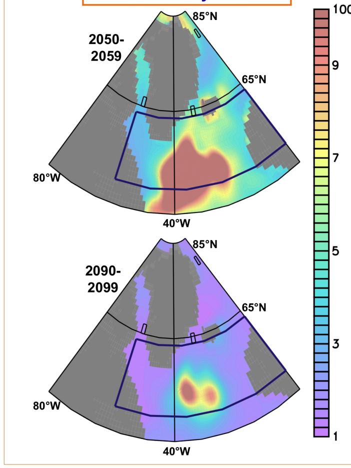

Future work/for discussion

- **Extend analysis to the full set of CMIP5 models.**
- **Clarify why uncertainty in model representation of the NASPG does not manifest closer to Greenland**
- **Analyze mechanisms underlying NASPG uncertainty in models (interaction with MOC and convection?).**
- **Weight/exclude individual models by their agreement with present day circulation/hydrography, including mean conditions and variability. Plausible criteria include:**
  - **Global mean surface temperature (Hawkins and Sutton 2009)**
  - **Global mean subsurface ocean temperature (Yin et al. 2011)**
  - **NASPG/MOC variability**
  - **Representation of critical model physics (e.g. aerosols)**
- **Assess means to relate GCM forcing in "source" regions to the ice interface**

References

Rignot, E., I. Fenty, D. Menemenlis, Y. Xu, Spreading of warm ocean waters around Greenland as a possible cause for glacier acceleration, Ann. Glaciol. 53(60), 257-266.

Straneo, F., D. A. Sutherland, D. Holland, C. Gladish, G. Hamilton, H. Johnson, E. Rignot, Y. Xu, M. Koppes, 2012: Characteristics of ocean waters reaching Greenland's glaciers. Annals of Glaciology, 53(60), 202-210.

Chang, Y. -S., S. Zhang, A. Rosati, T. L. Delworth, and W. F. Stern (2013), An assessment of oceanic variability for 1960-2010 from the GFDL ensemble coupled data assimilation, Clim. Dyn., 40(3-4), 775-803.

Acknowledgements

We are grateful for financial support from the Science, Technology and Environmental Policy program in the Woodrow Wilson School of Public and International Affairs at Princeton University and the Carbon Mitigation Initiative in the Princeton Environmental Institute. Thanks to GFDL and PCMDI for data and analysis tools, and to Olga Sergienko, Fiamma Straneo and Joe Majkut for helpful discussions.